

## THE NMC REGIONAL ANALYSIS SYSTEM

G.J. DiMego  
NOAA, NWS, National Meteorological Center  
Washington, DC, U.S.A.

### 1. INTRODUCTION

On 27 March 1985, the National Meteorological Center (NMC) implemented the new Regional Analysis and Forecasting System (RAFS). The purpose of the RAFS is to provide improved short-term numerical guidance. The principal emphasis is on improved prediction of quantitative precipitation and of significant weather events.

The RAFS is comprised of a hemispheric analysis which utilizes the method of optimum interpolation (OI). The analysis is followed by a non-linear normal mode initialization (Baer and Tribbia, 1977). The initialization is performed with a special hemispheric version of NMC's operational spectral forecast model (Sela, 1980) run with 80 wave resolution and 16 layers. The initialization is followed by a 48-hour prediction with the Nested Grid Model (NGM, Phillips, 1979 and Hoke, 1984). The NGM utilizes three nested grids. The outermost grid covers the hemisphere with a resolution of 366 km and the innermost grid covers North America with a resolution of 91.5 km (at 60N).

This paper will describe the Regional Optimum Interpolation (ROI) analysis component of the RAFS. The following section will describe the general characteristics of the ROI. Section 3 will discuss details of the preparation of the data and first guess, Section 4 will discuss quality control procedures, Section 5 will discuss details of the analysis, Section 6 will describe the performance of the analysis, and Section 7 will be a summary.

## 2. CHARACTERISTICS OF THE ROI

During the planning stages for the ROI, four modest goals were established for the new analysis: 1) improved resolution, especially in the vertical, 2) improved treatment of terrain, 3) improved mass-motion balance, and 4) improved utilization of the observed data. Improvement was measured relative to NMC's operational practices and performance at the time, and especially to the Limited-area Fine Mesh (LFM) system.

The horizontal analysis grid has dimensions of 180 by 60, with a resolution of approximately 2 degrees of longitude and 1.5 degrees of latitude, covering the Northern Hemisphere. Figure 1a depicts a portion of this grid over the central United States. Also shown for comparison are the LFM grid, Figure 1b, and the NGM C-grid, Figure 1c. Clearly, the resolution in the ROI analysis is comparable to the LFM. There still remains a considerable discrepancy between the resolution of the analysis and the innermost C-grid of the NGM. It is felt that any further increase in resolution would not be justified for two reasons. First, there is insufficient data to justify a resolution less than 150 km with an average spacing of radiosondes over North America at about 300 km. Second, the spectral resolution of 80 waves (rhomboidal truncation) in the initialization represents an upper limit on information transfer between the analysis and the model. It is felt that we are already at this upper limit.

The vertical coordinate of the RAFS is sigma, which is pressure normalized by the surface pressure at terrain level. This structure is depicted in Figure 2. There are 16 sigma layer mid-points carried in each component of the RAFS. By comparison, there are only 7 levels in the LFM forecast model and only 12 in the spectral model. The LFM analysis is performed on 10 mandatory pressure surfaces. The OI analysis for the global operational

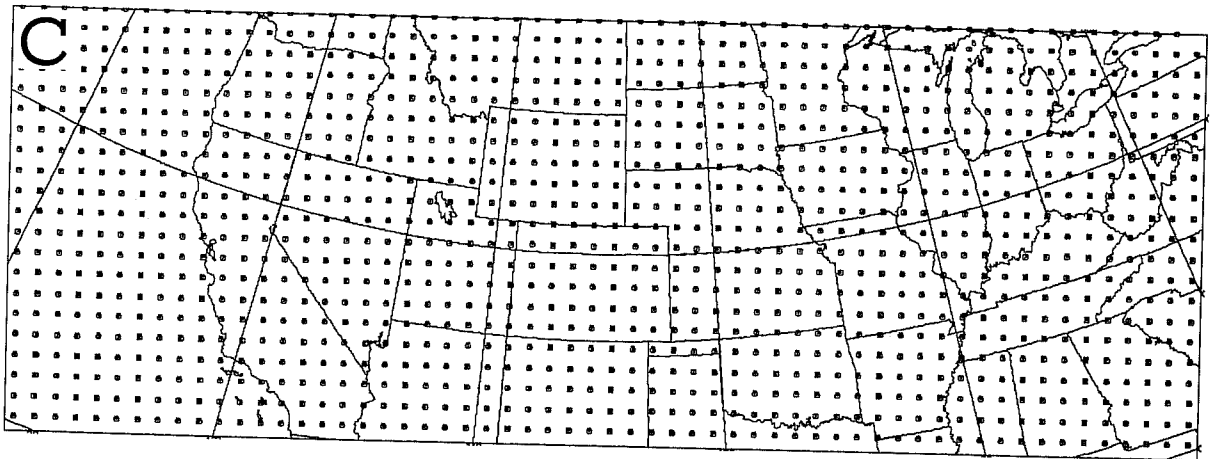
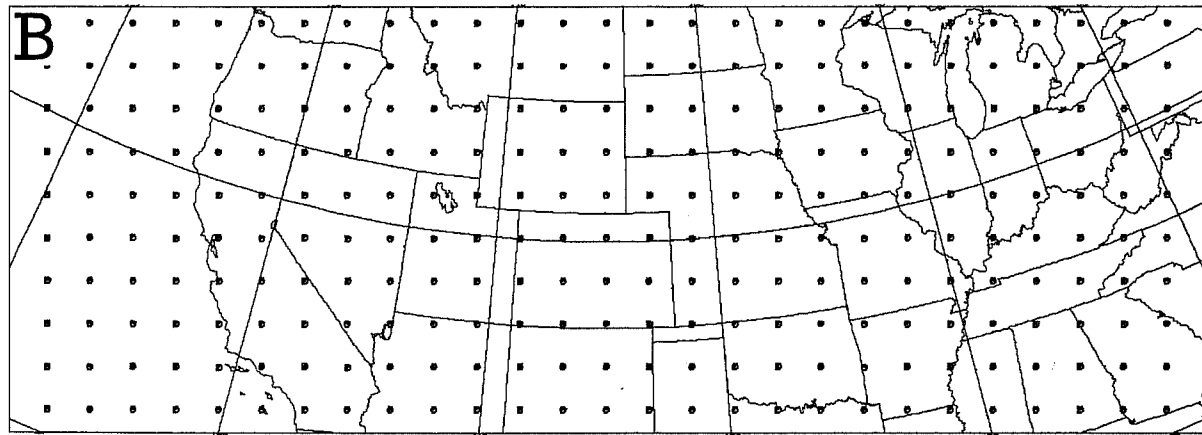
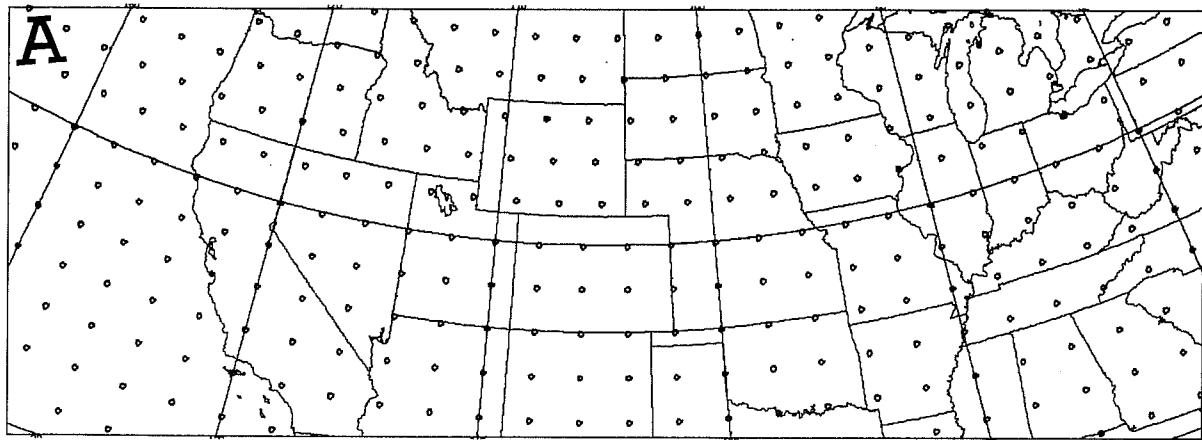


Figure 1. Portions of the ROI analysis grid (A), the LFM grid (B) and the NGM C-grid (C).

# MODEL STRUCTURE

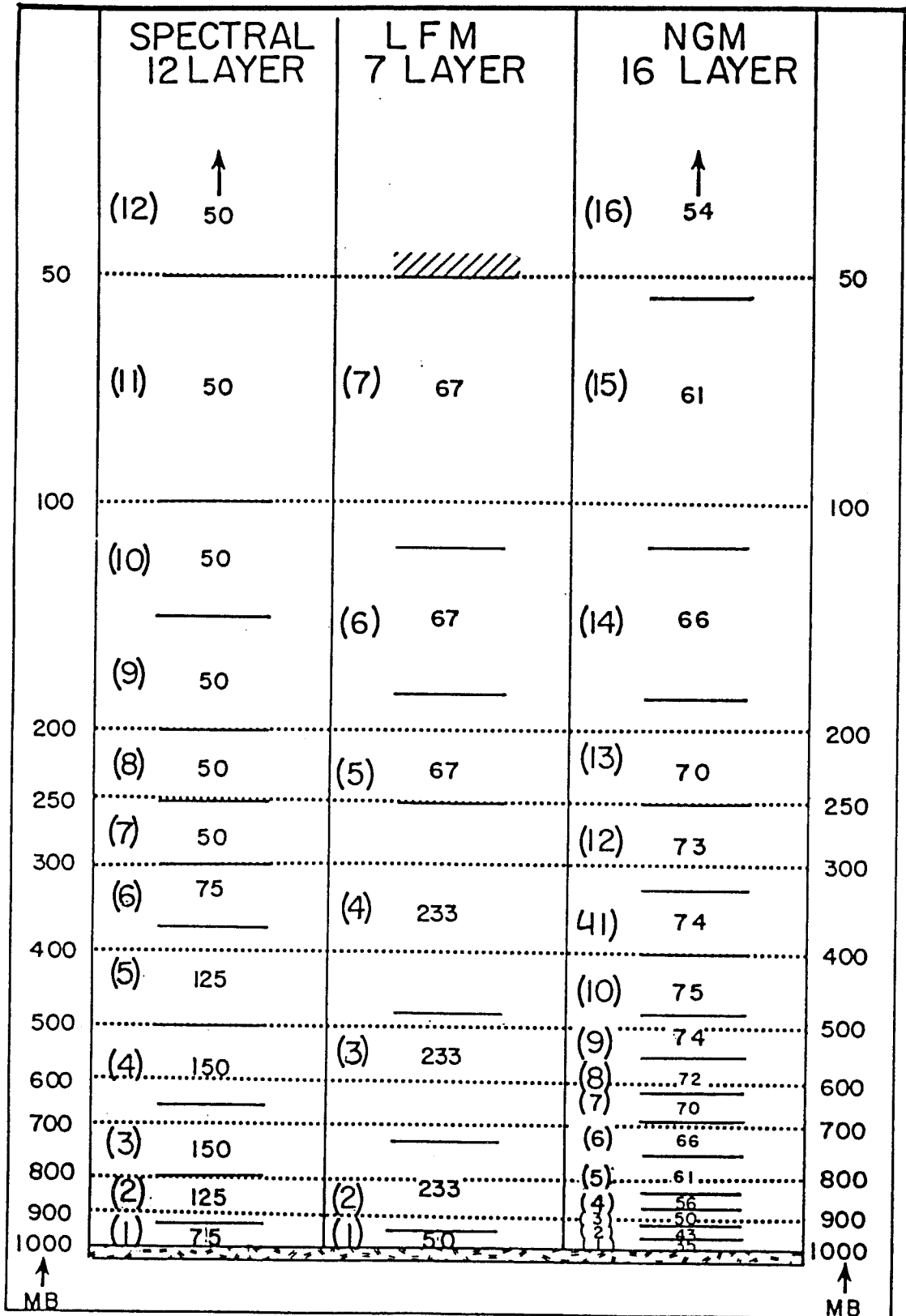


Figure 2. Vertical structure of the NMC prediction models: left, Global Spectral (GSM); middle, LFM; right, Nested-Grid Model. Solid lines refer to interfaces of the sigma layers which are numbered in parentheses and whose pressure depths are indicated in mb.

run and the OI analysis for the Global Data Assimilation System (GDAS) are both performed on 12 mandatory pressure surfaces. The ROI is performed at 16 levels in sigma. Clearly, the advantage lies with RAFS, especially in the troposphere where there are 12 levels below 250 mb.

The choice of sigma as the vertical coordinate in the analysis was determined by goal 2 from above and the distribution of levels in the NGM. The incorporation of terrain and boundary layer effects is more straightforward when dealing with a terrain-following coordinate. One could perform the analysis on pressure surfaces, as is done in other analyses at NMC, and transform into the sigma coordinate of the model via interpolation after the fact. However, this would result in considerable vertical smoothing unless there was sufficient resolution in the pressure profile to match the resolution in the desired sigma profile. To minimize this smoothing, analyses would need to be performed at roughly 50 mb intervals. Even at this resolution, there would still be some loss of detail in going from pressure to sigma because of the variations in the mid-point pressures due to sloping terrain. In addition, more analysis levels would be required at a 50 mb resolution than with sigma. Thus, for reasons of simplicity, efficiency and accuracy, the sigma coordinate was chosen for the analysis.

The LFM analysis, based on the method of successive corrections (Cressman, 1959) in two dimensions, contains only a loose coupling between the mass and wind fields. At times, ageostrophic features of an unrealistic nature can result, especially at and above the level of the jet stream. As recently reported by Dey and Morone (1985), the use of a strict multivariate OI analysis scheme based on geostrophically related forecast error correlations can produce analyses which are quite balanced and which require only modest changes by a non-linear normal mode initialization. This

procedure (hereafter denoted as GOI for Global OI) is now used in NMC's global analyses for the operational run and the GDAS. The ROI, having been developed more or less concurrently with the GOI, has adopted this approach.

There are two other advantages to the OI. First, the OI is three-dimensional. This insures that analyses will be more vertically consistent. This also facilitates the use of single level data, allowing their influence to be distributed vertically. Second, the OI provides a framework within which data of varying type and quality can be accommodated. This is important because of the hemispheric nature of the ROI domain.

The mathematical formulation of the ROI analysis is identical to that presented for the GOI; Dey and Morone (1985), Section 2c, Appendix A and Appendix B. However, in order to facilitate discussion of major differences in the application of OI between the two, a condensed description of this formulation will be given here.

The general form of the analysis equation can be written:

$$A_{gp}^a = A_{gp}^g + \sum_{i=1}^N W_i B_i^c, \quad (2.1)$$

where A is either h (geopotential), u (zonal wind), v (meridional wind), or q (specific humidity). Subscripts 'gp' denote a value at an analysis grid point, and 'i' at observation locations. Superscripts 'a' denote the analysis value, 'g' the first guess value, and 'c' an observed correction value. The B's represent the difference between an observed value and the first guess value and are the observed corrections. The W's are the computed weights given to each observed correction. The summation is over N observations suitably selected from a three-dimensional volume surrounding the grid point. In this way, the analyzed value is the simple sum of

the first guess and a linear combination of observed corrections to the first guess.

The analysis of  $h$ ,  $u$  and  $v$  is multivariate, such that the weighted sum will involve some combination of  $h$ ,  $u$  and  $v$  corrections. The same combination will be used for each analysis variable at a given point, which is required for balanced analyses. The limiting value of  $N$  for upper levels of the ROI analysis is 30. Up to 36 values can be selected at the first analysis level and up to 33 at the second. This allows for the increased density of surface observations.

It should be noted that the ROI specifies the vertical location of the analysis points in terms of pressure in the same way as the GOI. These values are simply computed at each point from the value of  $\sigma$  and the first-guess surface pressure. While the analysis pressures on a given level are fixed at the mandatory surfaces in the GOI, they vary from point to point in the ROI. As is discussed in Section 5, this impacts only the selection algorithm of the analysis, and not the mechanical application of OI.

The moisture variable analyzed in the RAFS is specific humidity as opposed to relative humidity in the GOI. The analysis is still univariate, but a limiting value of 10 is used for  $N$ . Analyses are generated at the first 12  $\sigma$  level mid-points of Figure 2, compared to 6 levels (1000-300 mb) in the GOI. The doubling of the vertical resolution for moisture has been made possible by the use of significant level data (see section 4).

The calculation of the weights,  $W_i$  in Equation (2.1), involves the solution of a system of  $N$  simultaneous linear equations derived by minimizing an

expression for the mean-square error of the analysis. This system, or matrix, can be written in normalized form as:

$$\sum_{j=1}^N \{ \rho_{B_i B_j}^{tc tc} + \rho_{B_i B_j}^{oe oe} \epsilon_i \epsilon_j \} w_j = \rho_{B_i A_{gp}}^{tc tc},$$

$$i = 1, N,$$
(2.2)

where

$$\rho_{B_i B_j}^{tc tc} = \frac{\overline{B_i^{tc} B_j^{tc}}}{[(B_i^{tc})^2 (B_j^{tc})^2]^{1/2}},$$
(2.3a)

$$\epsilon_i = \frac{[(B_i^{oe})^2]^{1/2}}{[(B_i^{tc})^2]^{1/2}},$$
(2.3b)

$$w_j = \frac{[(B_j^{tc})^2]^{1/2}}{[(A_{gp}^{tc})^2]^{1/2}} W_j.$$
(2.3c)

The first correlation on the left-hand side of (2.2) involves the correlation of the 'true' first-guess correction between observation  $i$  and observation  $j$  (2.3a). The second involves the correlation of observation errors at  $i$  and  $j$  and is multiplied by factors (2.3b) relating the observational error standard deviation to the 'true' correction standard deviation. The correlation on the right-hand side involves the correlation of the 'true' correction for observation  $i$  and the analysis variable at the grid point. The relationship between the normalized weights,  $w$ , and the un-normalized weights,  $W$ , is given by (2.3c).

In the ROI, as in the GOI, the autocorrelation between 'true' first-guess corrections of geopotential is modeled. It may be written as:

$$\rho_{h_i h_j} = \mu_{h_i h_j} \nu_{h_i h_j} = \overline{h_i h_j} / \sigma_{h_i} \sigma_{h_j}$$
(2.4)



where  $\sigma$  is the standard deviation of the first-guess height corrections,

$$\mu_{h_i h_j}^2 = \exp(-k_h S_{ij}^2), \quad (2.5)$$

is the horizontal factor of the three-dimensional correlation, and

$$v_{h_i h_j} = \frac{1}{1 + k_p \ln^2(P_i/P_j)}, \quad (2.6)$$

is the vertical factor. Here,  $P$  is pressure and  $S_{ij}$  is the separation distance between points  $i$  and  $j$ . The distance approximations for  $S$  can be found in Dey and Morone (1985) (Equation 2.10a for the points equatorward of 70N and Equation 2.10b for points poleward of 70N). The constants  $k_h$  and  $k_p$  control the rate at which the correlation decreases with horizontal and vertical distance, respectively.

All correlations which involve geopotential and wind or wind and winds are now calculated from (2.5) and (2.6) assuming a geostrophic coupling between the  $h$ ,  $u$  and  $v$  correlations. These expressions are given in Appendix A and B of Dey and Morone (1985). This does not mean that the analyses are geostrophic. Only the corrections to the first guess are constrained to be geostrophic and only outside of the tropics.

The remaining parameters needed to solve (2.2) are the standard deviation of the first-guess corrections, the standard deviation of observational errors and the correlation of observational errors. Their treatment follows that of the GOI. Where there are differences, they will be noted in Section 5. The system (2.2) is solved at each point for each analysis variable by an iterative technique based on the method of conjugate gradients (Beckman, 1960).

The next three sections will describe the ROI procedures in some detail. To facilitate the discussion, the steps involved in the ROI are depicted

schematically in Figure 3.

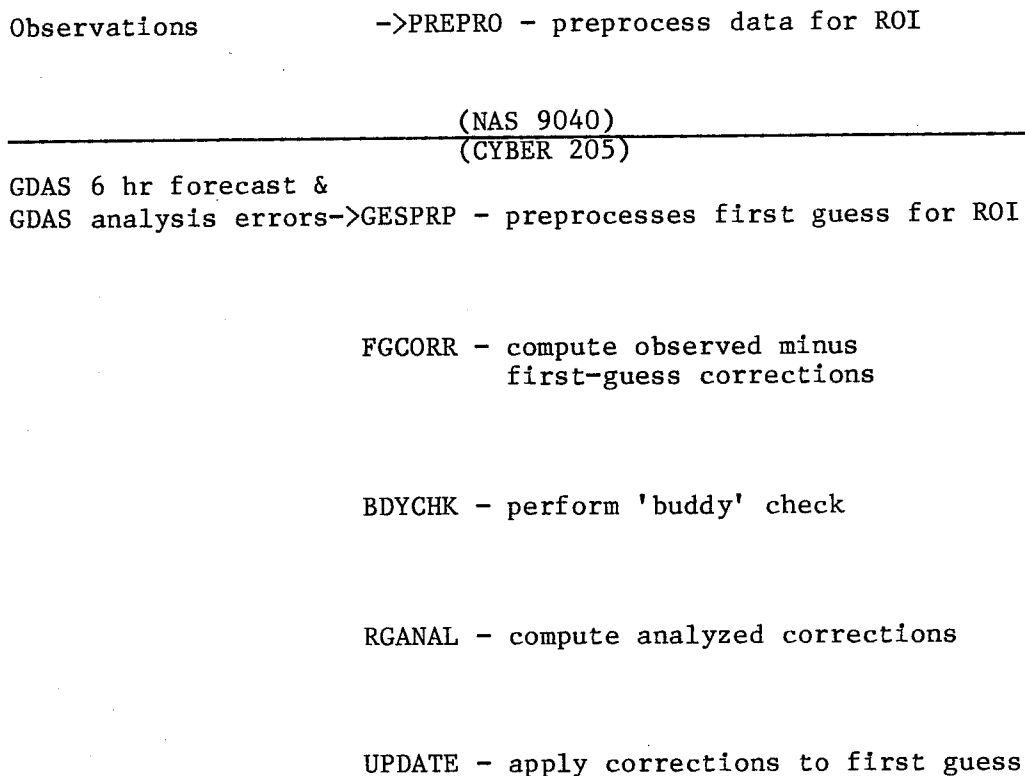


Figure 3. Schematic of steps involved in the RAFS optimum interpolation analysis.

### 3. PREPARATION OF DATA AND FIRST GUESS

The basic function of the OI data preprocessor is to construct the database for the analysis. This involves combining data from various sources, selecting the information required by the analysis, performing rudimentary checks for time, location, completeness and quality, converting units, applying corrections, and putting the information in the format expected by the analysis.

Preprocessing is performed on the front-end Hitachi NAS 9040 computer system (Figure 3). This facilitates the unpacking of data which are in various formats on the front end. The packed output format minimizes the volume of information which is transmitted across the data link to the

Control Data Corporation CYBER 205. Observations are read in, processed and written out one report at a time. The following sub-sections will deal with the various types and sources of data used in the ROI analysis.

### 3.1 Radiosondes, dropsondes, and pibal wind profiles

Consistent with Goal 4 of Section 2, all significant level data are incorporated in the ROI. Both the LFM and the GOI analyses utilize only mandatory level data. Of course, the analyses are performed at those levels and the models which they support have roughly comparable vertical resolution: 10 (12) analysis levels versus 7 (12) model layers for the LFM (global system). Again, it is the fine resolution of the RAFS sigma coordinate which provides both the impetus and justification for including all of the vertical structure from the sounding data.

Profile reports are processed in the following manner. First, the mandatory level information is combined with the significant level temperature data. Specific humidity,  $q$ , is calculated and temperature,  $T$ , is converted to virtual temperature,  $T_v$ . Geopotential heights,  $h$ , are integrated to the significant levels. Next, the wind components,  $u$  and  $v$ , are computed from the speed and direction. The wind levels are then merged with the existing profile. Temperature and moisture are generated at wind-only levels and winds are generated at mass-only levels by linear interpolation with respect to the natural logarithm of pressure,  $\ln p$ . Geopotential heights at the wind-only levels are also generated by hydrostatic integration. This process results in a merged profile where each level has a complete set of variables,  $p$ ,  $h$ ,  $T_v$ ,  $q$ ,  $u$ , and  $v$ .

During this merging process, values are generated at certain fixed pressure levels. If the profile contains significant level information, then data

levels every 25 mb are generated. If only mandatory level information is reported, then data levels every 50 mb are generated. While many of these levels may not have been actual reporting levels, it is felt that since interpolation is performed between the reported values, the basic features of the observed sounding are preserved. In any event, the complete profile, including mandatory, significant and generated levels, is packed and made available for processing by the ROI codes on the CYBER 205.

Prior to the merging process, all daylight sounding data are corrected for the effects of shortwave solar radiation on the temperature instrument. The corrections of McInturff et al. (1979) are tabulated for height and temperature by mandatory pressure level, solar elevation angle and instrument type. All levels from 700 mb and above are corrected. Significant level temperature corrections are determined by interpolation within the table.

### 3.2 Satellite temperature profiles

Profiles of temperature from polar-orbiting (TIROS) and geostationary (VAS) satellites are processed in the following manner. The reported temperatures are processed into profiles of geopotential thickness. All layers are relative to a base level of 1000 mb where the geopotential is set to zero. Values of level virtual temperature and layer thickness are derived at 23 pressure levels, every 50 mb from 1000 mb to 50 mb plus 70 mb, 30 mb, and 20 mb. At present, VAS retrievals are not being processed operationally. In addition, no TIROS retrievals over land nor microwave retrievals south of 20N are used. A recent upgrade of the ground processing system for the polar-orbiting data has resulted in almost all relevant orbits being available to the ROI by its data cutoff of 2.25 hours after synoptic observation time (0000 GMT and 1200 GMT).

### 3.3 Moisture bogus profiles

The National Environmental Satellite Data and Information Service (NESDIS), provides NMC with a set of moisture bogus data twice a day (0000 GMT and 1200 GMT). From 400-500 points are provided covering the eastern Pacific and western Atlantic at a resolution of about 250 km. At each point, a code figure (1-13) is provided which corresponds to a characteristic profile of relative humidity, RH. The preprocessor converts this code into values of RH at 12 pressure levels. The data values prescribed are listed in Table 1.

Table 1. Code - relative humidity (%) equivalents for moisture bogus

Code (mb)	1	2	3	4	5	6	7	8	9	10	11	12	13
300	75	55	53	34	10	10	10	10	70	10	10	70	70
400	85	74	67	44	50	10	10	10	70	10	20	70	70
500	90	83	67	54	85	20	25	15	25	10	85	32	85
600	93	85	72	58	68	49	38	20	25	10	88	41	55
650	94	86	74	60	59	64	44	23	25	10	89	46	40
700	95	87	76	62	50	79	50	25	25	10	90	25	25
750	96	89	80	65	48	84	63	39	36	19	91	63	34
800	97	91	83	67	44	88	76	52	48	27	92	76	42
850	98	93	86	70	39	92	89	65	60	35	92	89	50
900	97	92	84	71	50	90	85	67	63	39	91	85	56
950	96	91	82	72	59	87	80	70	66	42	90	80	62
1000	95	90	80	72	68	84	76	73	69	45	90	76	68

### 3.3 Single level wind data

Conventional aircraft data (AIREP's), Automated Satellite Data Relay (ASDAR) aircraft data, and ARINC Communications Addressing and Report System (ACARS) aircraft data are processed as single level data. In addition, satellite cloud-drift wind reports are included from all geostationary satellites which reach NMC by the data cutoff time. Only the wind data, converted to u and v, are used. If necessary, the reported pressure altitude is converted to pressure. There is no attempt to distribute these winds to fixed pressure levels. The observation is considered at its reported level by the ROI.

### 3.4 Surface data

Marine surface data sources include fixed and mobile ships, moored and drifting buoys, and manual bogus reports. When reported, temperature and dew-point are used to compute virtual temperature and specific humidity. The reported sea-level pressure is used directly with an appropriate geopotential of zero for mean sea-level. As discussed by Bergman (1979), all oceanic surface winds are adjusted to be pseudo-geostrophic using a marine boundary layer adjustment. A check is performed to insure that no marine surface reports occur over land.

Surface reports over land are included in the ROI, as opposed to the GOI which excludes them. Values of surface (station) pressure and reduced sea-level pressure are used when both are reported. This is a common practice for most stations in North America. Surface values of virtual temperature, specific humidity and geopotential (station elevation) are provided when reported with a surface (station) pressure. When only reduced sea-level pressure is reported, no other information is included with that pressure. No wind data are used from surface land reports at this time. In addition, surface land reports must be within +/- 1.5 hours of analysis time, as compared to +/- 3.0 hours for all other types of data.

### 3.5 Quality code assignment

As observations are processed into the NMC database, certain automated consistency checks are performed. The results of these checks are coded along with the data values and are available to the ROI data preprocessor. A description of these checks and other aspects of data handling and quality control can be found in DiMego et al. (1985). The preprocessor examines these various quality indicators and assigns the appropriate ROI quality code, see Table 2. Any observed value which either failed the

consistency check or was 'purged' by the monitor is removed from further consideration by the ROI. Unfortunately, the early data cutoff time of 2.25 hours for the ROI does not allow much time for subjective evaluation of the data by the monitor. Therefore, a heavy reliance is placed upon automated checking procedures.

Table 2. Quality codes for the ROI analysis

ROI Code	Meaning
0	Monitor requests observation be kept
1	Correct, passed consistency checks
2	Probably correct, not checked
3	Suspect, passed with loose limits

### 3.6 Preparation of first guess

The first guess fields for the ROI are provided by the Global Data Assimilation System which consists of a 6-hour forecast with a 30-wave 12-layer spectral model. Also provided are the analysis error standard deviations from the GOI that generated the initial conditions for the forecast. The preparation of the latter will be discussed first, followed by a description of the processing of the first guess fields.

The analysis error (actually their natural logarithms) are in spherical harmonic form on the GOI analysis levels, i.e. 12 mandatory pressures. The first step is to decompose the spectral coefficients onto the ROI analysis grid-points. The profile of errors at each point is then interpolated vertically assuming a linear variation with respect to  $\ln p$ . The pressures to which the interpolation is performed are computed at each point from the first guess field of surface pressure. Geopotential and wind errors are interpolated to the first 16 ROI sigma interface pressures. The RH errors are provided at the first 6 pressure levels and are interpolated to the

first 12 sigma mid-point pressures.

For the geopotential errors, the profile is first adjusted such that values increase upwards. This allows an estimate of the temperature error to be calculated by vertical differentiation of the height error profile, although this field is no longer required by the ROI. This reflects that fact that the original ROI analyzed temperature instead of geopotential. However, the balance between the mass and wind fields generated by this preliminary version of the analysis was judged to be too weak, especially when compared to that which can be achieved using a strict coupling of geopotential and wind.

Although it is performed in the analysis code, it is convenient to discuss at this point the process by which these analysis errors are converted into standard deviations of the first-guess corrections. As discussed by Dey and Morone (1985), this is achieved by adding an appropriate error growth rate to the analysis error standard deviations. This error growth rate is only a function of the variable, sigma level and range of the forecast. The values currently used are listed in Table 3. Values have been roughly determined from those given in Dey and Morone (1985) for height, and from values previously used for wind.



Table 3. Forecast error growth for a 6-hour forecast period, with minimum allowed values in parentheses

Level	(mb)	h (m)	u&v (m/s)
16	( 54)	15 (50)	1.80 (4.0)
15	( 115)	17 (40)	1.80 (5.0)
14	( 181)	18 (33)	2.00 (5.6)
13	( 251)	18 (28)	2.20 (6.0)
12	( 324)	18 (18)	2.35 (6.0)
11	( 398)	16 (15)	2.35 (5.4)
10	( 473)	13 (14)	2.20 (4.8)
9	( 547)	10 (13)	2.10 (4.1)
8	( 619)	9 (12)	1.95 (3.5)
7	( 689)	8 (12)	1.75 (2.9)
6	( 755)	8 (12)	1.75 (2.5)
5	( 816)	8 (12)	1.60 (2.2)
4	( 872)	8 (12)	1.60 (2.0)
3	( 922)	8 (12)	1.60 (2.0)
2	( 965)	8 (12)	1.60 (2.0)
1	(1000)	8 (12)	1.60 (2.0)

Values for the wind component errors are listed as well because they are used in the tropics. The GOI uses a fixed profile of wind errors in the tropics (Table 4 of Dey and Morone). In higher latitudes, the values used for u and v are computed from h in the same way as is done in the GOI. This is in accordance with the strict application of a geostrophic covariance model. Observed and computed values are blended using the coefficient of geostrophy in the transition zone from 25N to 10N.

Also listed in Table 3 are the minimum values allowed for the standard deviation of the first-guess corrections. This limit is applied after the analysis errors are inflated by the error growth rate. There is no limit on the maximum value, since a limit based on the climatological error variance has been applied by the GOI.

The minimum values presented are slightly larger than the observational error standard deviations for radiosonde data (Table 5 of Dey and Morone). The intent here is to insure that the first guess fields do not appear

better (statistically) than the observed data. This reflects our discomfort with the procedure for obtaining the first guess errors. Ideally, the initial error pattern would not only grow with time but also evolve spatially through the forecast period. This evolution would probably resemble the evolution of the actual forecast parameters. At this time, only a static growth of the initial error is accounted for.

The first guess field coefficients include surface pressure ( $P^*$ ), model terrain ( $Z^*$ ), 12 sigma mid-point levels of virtual temperature ( $T_v$ ), vorticity and divergence, and 7 mid-point levels of specific humidity. The wind components,  $u$  and  $v$ , are computed in spectral form from the vorticity and divergence. Each field is then decomposed onto the ROI analysis grid-points. Geopotential values at the input interface pressures are obtained by direct integration of the temperatures which are interpreted as mean layer values.

At this point, a field of high-resolution terrain is read in. The field is already on the ROI grid and was generated from a 1 degree by 1 degree field which was computed by fitting spherical harmonics with 72 wave resolution (triangular truncation) to a highly detailed terrain data set. This field is incorporated in the output fields by computing a new  $P^*$  valid at the new  $Z^*$  from the first guess profiles of height and temperature. This is performed assuming that height varies quadratically with respect to  $\ln p$  (Gerrity, 1977). The formulation involves values of height and temperature at the levels which bracket the new  $Z^*$  level. An estimated value of the surface virtual temperature,  $T^*$ , is computed hydrostatically at the original  $Z^*$  level and is used whenever the new  $Z^*$  falls below the second interface. It is also used whenever extrapolation is required below the first interface (original  $Z^*$  level).

The new  $P^*$  field is used to compute the mid-point and interface pressures of the ROI. Vertical interpolation from the 12 input levels to the 16 output levels proceeds as follows. For geopotential, the profile of interface heights is interpolated to both mid-point and interface pressures using an iterated AITKEN interpolation scheme which is of variable order in  $\ln p$  (Conte, 1965). This profile is then checked for superadiabatic lapse rates between successive layers (involving three height values). The procedure is iterated until all adjacent layers are adiabatic. The adjustment insists that the total thickness of the two layers be conserved. Therefore, only the middle value of height is changed. The 16 mid-point values of geopotential are stored and 16 mid-point temperatures are computed from the thickness of successive interface values. A new  $T^*$  value appropriate to the new  $P^*$  and  $Z^*$  is computed from the thickness between the first interface ( $Z^*$ ) and the first mid-point. The wind components (specific humidity) are interpolated to the 16 (12) mid-points assuming linear variation with respect to  $\ln p$ . A complete set of variables,  $P^*$ ,  $Z^*$ ,  $T^*$ ,  $Z$ ,  $T_v$ ,  $u$ ,  $v$ , and  $q$ , is now available on the ROI grid.

### 3.7 Preparation of observed corrections to the first guess

The next step is to construct the set of observed corrections to the first guess. The prepared data are read in and stored together with the first guess fields. When dealing with profile reports, only the data at fixed pressure levels are stored. This amounts to 36 levels at a frequency of every 25 mb or 23 levels at a frequency of every 50 mb. The observations are next sorted into 2.5 degree latitude bands and ordered by increasing longitude within each band.

During the sorting process, all single-level data are examined for possible combination into 'super' observations. The criteria for two (or more)

reports to be combined are that they must be within 1.0 degrees of latitude, must be within 1.2 degrees of longitude, must be within 12.5 mb (25 mb for upper levels winds) and must be of the same report type (aircraft with aircraft, surface with surface, etc.). The 'super' observation is constructed by forming the linear average of time, location, pressure and observed values. This procedure is not as elegant as that of Lorenc (1981), but is effective in reducing the volume of data and increasing its representativeness. The ROI quality code is decreased (improved reliability) to reflect the latter. In addition, the geographical limits are increased outside of North America where the resolution of the analysis is decreased (see Section 5).

First guess values are now computed at each observation location. Horizontal interpolation is bi-linear in x and y. Vertical interpolation is linear with respect to  $\ln p$  for the variables  $T^*$ ,  $u$ ,  $v$  and  $q$ . Geopotential is interpolated quadratically in  $\ln p$ . Extrapolation below the first guess terrain is limited to be within 50 mb (except for 1000 mb height). The estimated first guess value of surface temperature,  $T^*$ , is used for mass variables falling below the first sigma mid-point. Extrapolation above the top sigma mid-point is allowed only for winds and only if they are within 5 mb. A first guess value of 1000 mb height is computed from surface values  $P^*$ ,  $Z^*$  and  $T^*$  using the reduction procedure known as 'SHUELL' (Gerrity, 1977).

All that remains is to calculate the difference between the observed values and the interpolated first guess values. This quantity (observed-forecast) represents the observed correction to the first guess. Values of relative humidity from the moisture bogus profiles are converted to specific humidity values using the first guess temperature. Satellite thickness profiles are

converted to geopotential profiles by anchoring them to the first guess 1000 mb heights. All sea-level pressure observations are converted to values of 1000 mb height. This hydrostatic conversion uses the estimated below ground temperature obtained when the 'SHUELL' reduction procedure was applied to the first guess. With the single exception of surface temperature corrections from surface observations, all corrections to the first guess are now in terms of the analysis variables,  $h$ ,  $u$ ,  $v$  and  $q$ .

#### 4. QUALITY CONTROL PROCEDURES

There are two forms of quality checking within the ROI code. The first involves a 'gross' check on the magnitude of the observed corrections. This check is designed to reject reports which are nonmeteorological. The second is a consistency check where neighboring corrections are compared. This 'buddy' check is an inexpensive means of detecting corrections whose inclusion in the analysis would be detrimental. Both checks rely on the ROI quality codes listed in Table 2 to make decisions concerning acceptance or rejection.

##### 4.1 The 'gross' check

In the 'gross' check, each observed correction value is compared to an allowable limit on its magnitude. A fixed limit of 15 g/kg is used for specific humidity. The other limits are based on a table of representative standard deviations of first guess error compiled by variable, pressure and latitude band. The number of standard deviations allowed for a given correction is a function of the ROI quality code. These are listed in Table 4.

Table 4. Number of standard deviations allowed in 'gross' check for tossing and for flagging observed corrections

Data Type	Quality Code	Number of Standard Deviations	
		toss if >	flag if >
Non-surface Z, u, v	1	5.5 (7)	2.5 (3)
	2	4.5 (6)	2.5 (3)
	3	3.5 (5)	2.5 (3)
Surface	1-3	3.0 (4)	1.5 (2)

No values are given for a quality code of zero, because these reports were requested to be kept and are not allowed to be rejected. A flag is set on those reports which have questionably 'large' magnitudes as determined by the limits listed under 'flag' in Table 4. The looser limits listed in parentheses for both tossing and flagging are used for all North American radiosondes. This reflects their generally higher level of reliability and homogeneity. In addition, the looser limits for flagging are used for all 'super' observations. Limits for tossing reports are tightened if extrapolation was required to obtain a first guess value.

#### 4.2 The 'buddy' check

Prior to performing the analysis, all observed corrections which passed the 'gross' check are checked for internal consistency by step BDYCHK (Figure 3). For the purposes of data collection, an equal-area reference grid is used which has a resolution of 5 degrees at the equator. All reports within 7.5 degrees (or an equivalent distance) of each reference point are collected. The reports are sorted into groups of like variable (h, u or v), the 'buddy' check being univariate. The groups are also sorted by pressure layer where the layer mid-points are the mandatory pressure levels. In this way, the 'buddy' check is three-dimensional. For example, a profile report with data every 25 mb will contribute four levels (1000, 975, 950 and 925 mb) to the group for the first layer and six levels (900, 875,

850, 825, 800 and 775 mb) to the group for the second layer and so forth.

Each group with at least three observed corrections is subjected to the checking procedure discussed below. If there are only one or two values in a group, a check is made for any flagged reports. Recall that these reports were identified in the 'gross' check as having questionably large deviations from the first guess. Flagged values are excluded from further consideration by either the 'buddy' check or the analysis. This heavy handed approach reflects our lack of knowledge on how to adequately incorporate these isolated reports when they deviate so much from the first guess field. The rationale for deleting such reports is based on our experience with the GOI and GDAS that such observations can cause severe problems in the analysis and subsequent forecast.

For each group with three or more values, the correlation of the first guess error is computed for each pair of values in the group. This calculation is three-dimensional (Eq. 2.4 and 2.5) and involves only the autocorrelations  $\rho_{h_i h_j}$ ,  $\rho_{u_i u_j}$  and  $\rho_{v_i v_j}$ . Next, each pair of reports, R1 and R2, is compared and the magnitude of the difference of their corrections is normalized by the appropriate tabular value of first-guess error standard deviation. This normalized difference,  $|R1-R2|/\sigma$ , is compared to a limiting value which is a function of the First-guess Error Correlation (FEC) between the reports:  $DFMAX = [3.5 - 2.5*FEC]$ . If the normalized difference exceeds the limiting value, then TOSS flags are set. If the normalized difference is less than the limiting value, then 'KEEP' flags are set. This screening criterion is depicted schematically in Figure 4. In essence, if two reports have a low correlation (are far apart), then the limiting value is large. On the other hand, when two reports are highly correlated (close together), then the limiting value is

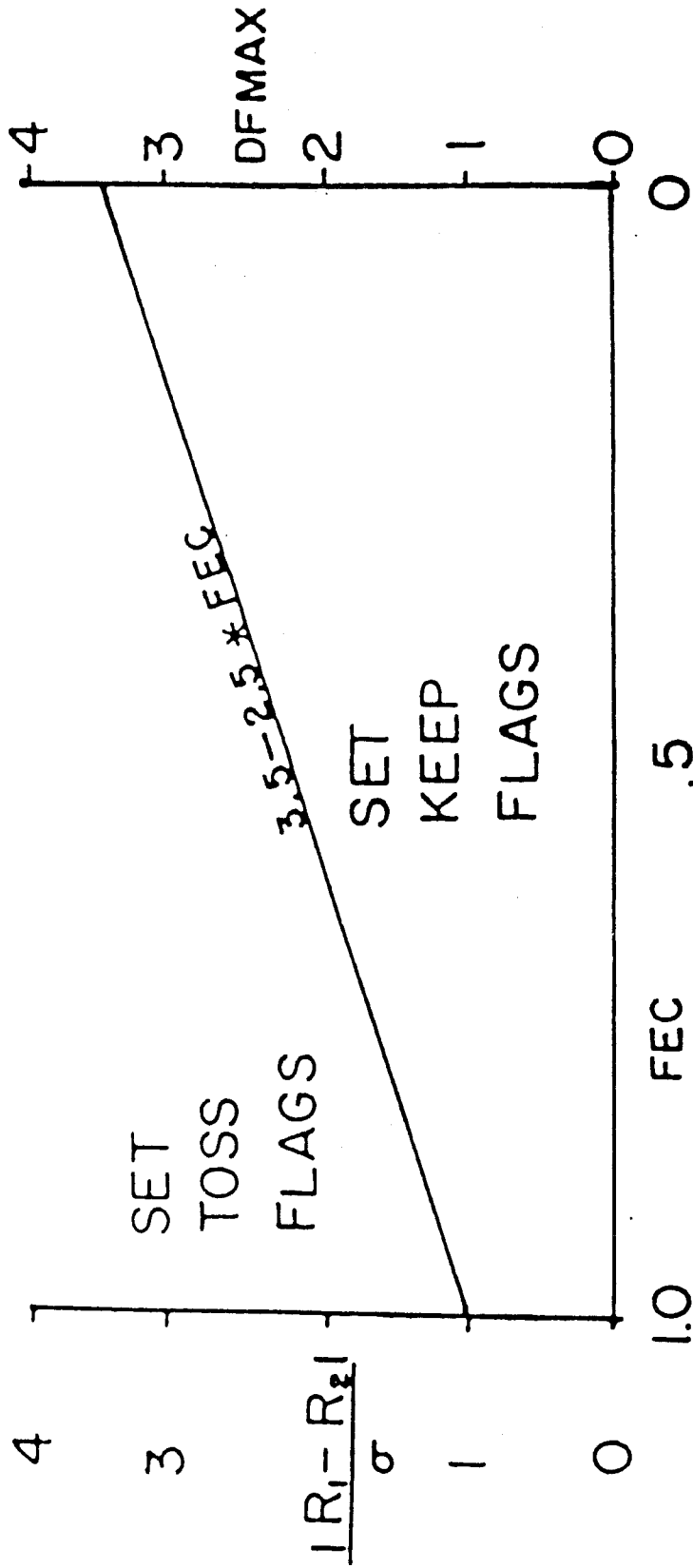


Figure 4. Schematic representation of screening criteria in 'buddy' check. FEC stands for forecast error correlation. Linear function for DFMAX marks separation of zones based on normalized magnitude of observed corrections  $R_1$  and  $R_2$ .



small and the corrections are expected to agree within at least one standard deviation.

The setting of 'TOSS' or 'KEEP' flags depends on the type of report and especially the ROI quality codes (Table 2). When setting 'TOSS' flags, the report with the larger quality code (less credibility) receives the 'TOSS' flag and the report with the lesser code receives no flag.

Correspondingly, when setting 'KEEP' flags, the report with the smaller quality code (more credibility) receives the flag. If the quality codes or the report types are equal, then both reports receive flags.

The total number of 'KEEP' and 'TOSS' flags accumulated by the report determines whether or not the report is eliminated from further consideration. Any value receiving two or more 'KEEP' flags is automatically retained. Reports with a quality code of zero are also retained unconditionally. Any report which has been flagged as questionably large and does not have at least two 'KEEP' flags is removed. The remaining reports in the group are examined and the report with the largest number of 'TOSS' flags (greater than two) is removed. Reports are eliminated one at a time and all flags which the offending report caused to be set are removed. The process is repeated until no reports remain with two or more 'TOSS' flags.

In conclusion, one should note that if a wind component is eliminated, its other component is removed as well. Unfortunately, if the v component is rejected, it is impossible at this point to eliminate any negative influence its corresponding u component might have had on the procedure. It is also clear that the entire process will not handle the case when there are three or more rogue reports which corroborated one another. Each would

receive at least two 'KEEP' flags and none would be eliminated.

## 5. THE ANALYSIS

The first function performed by the analysis code, step RGANAL, is to generate a 1000 mb analysis of geopotential corrections. This analysis is performed univariately over the full 180 x 60 ROI analysis grid. The data search is three-dimensional, selecting up to 16 reports from the vicinity of each grid point. This is the only application which utilizes the reduced sea-level pressure values which were converted to 1000 mb height corrections in step FGCORR. Height corrections at the lowest reported level of radiosonde or dropsonde reports are the other source of data. The selection is based on the magnitude of the three-dimensional first-guess error correlation. A value of  $k_h = 3.0 \times 10^{-6} \text{ km}^{-2}$  is used in Eq. 2.4 for the horizontal factor and a value of  $k_p = 9$  is used in Eq. 2.5 for the vertical factor.

This geopotential field is used for two purposes. First, the correction field is interpolated to the satellite profile locations and applied to the geopotential corrections at each level. Since these were anchored to the first guess 1000 mb height value, adding the correction effectively re-anchors the profiles to the analyzed 1000 mb height field. Second, a field of sea-level pressure is computed from the analysis by reversing the same 'SHUELL' reduction process which was used to generate the first guess 1000 mb height field and to convert sea-level pressure reports to 1000 mb geopotential.

The full ROI analysis grid is defined in terms of nearly fixed increments of latitude and longitude. Consequently, there is a large variation in the resolution in the zonal direction as one goes from equator to pole. A

thinned grid has been incorporated on which the corrections are analyzed. The thinning process involves two steps. First, the longitude increment is increased north of 40 degrees and the number of points in a grid row are decreased. The increment is computed to match the equivalent distance of 1.5 degrees of latitude. Second, areas outside of North America are further thinned to every other point in the zonal direction. The points which are dropped are staggered from one grid row to the next. The resulting grid is depicted in Figure 5. This second thinning is an attempt to account for the variation of data density, i.e. lack of data over the oceans, and to approximate the decreased resolution of the outermost grids of the NGM (366 km for the A-grid and 183 km for the B-grid at 60N).

Next, the upper level analyses of  $h$ ,  $u$  and  $v$  are performed. The first guess fields and error standard deviations are first interpolated to the analysis points on the thinned grid. Since the location of the grid rows has not been affected by the thinning, this involves only a linear interpolation in the zonal direction. The analysis proceeds from point to point along each grid row, analyzing all levels at a point before stepping to the next. Observed correction locations are collected up to a 15 degree (or equivalent distance) radius of the grid point in question. This radius can be less if sufficient (10) profile reports are found within a shorter distance.

At each level, the  $N$  observed corrections to be included in the actual analysis must be selected. Of the  $N$  values selected, 20 are allocated to profile reports and the remaining 10 (16 at the first level and 13 at the second) are allocated to single level reports. In addition, no more than two levels of height and no more than one level of  $u$  and  $v$  can be selected from the same profile report. The partitioning eliminates the possibility

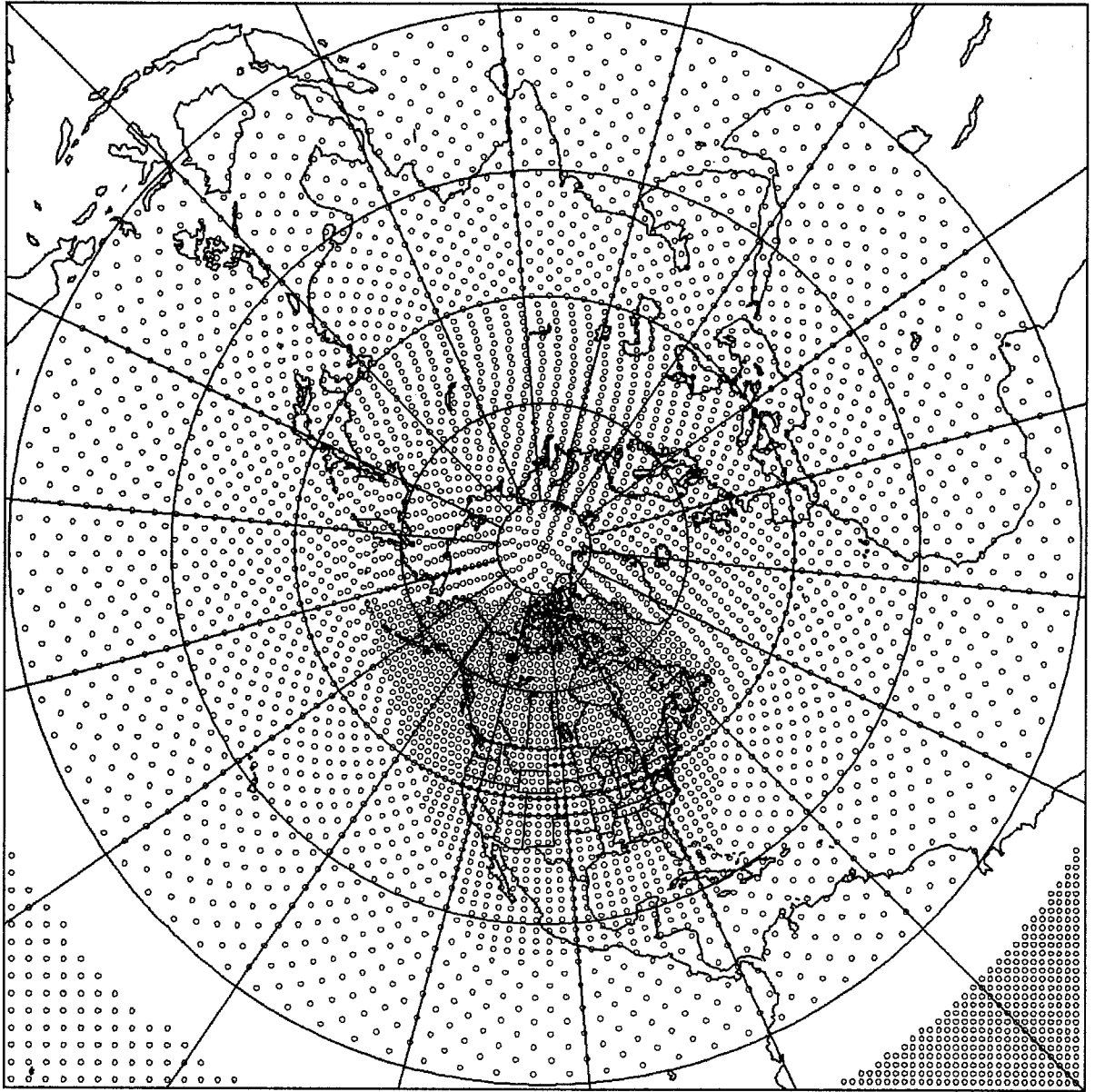


Figure 5. The ROI grid at which analyzed corrections are computed. The wedge of points in the lower left corner represents the NGM A-grid resolution. The NGM B-grid is in the lower right.

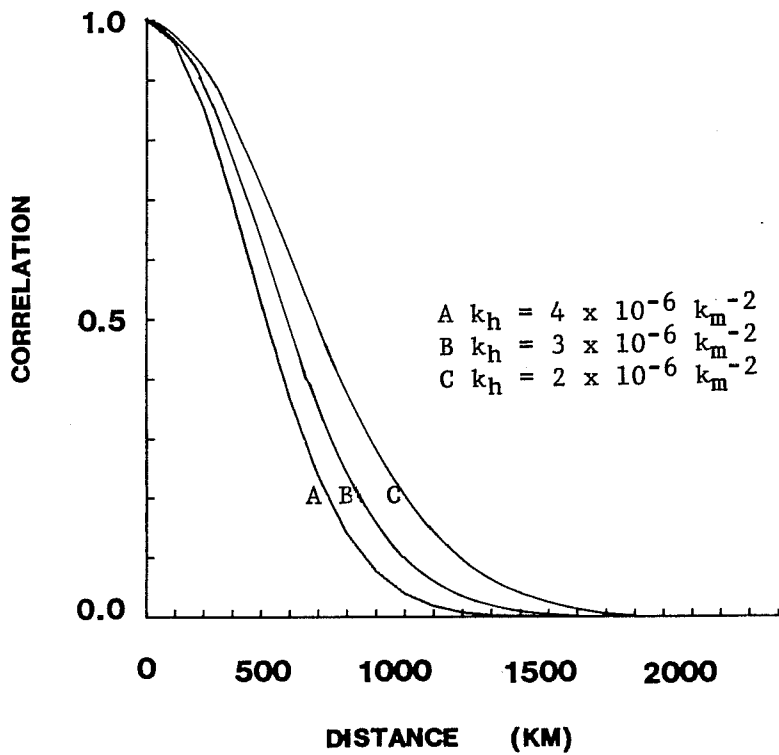


Figure 6. Horizontal first guess error correlation for selected values of  $k_h$ .

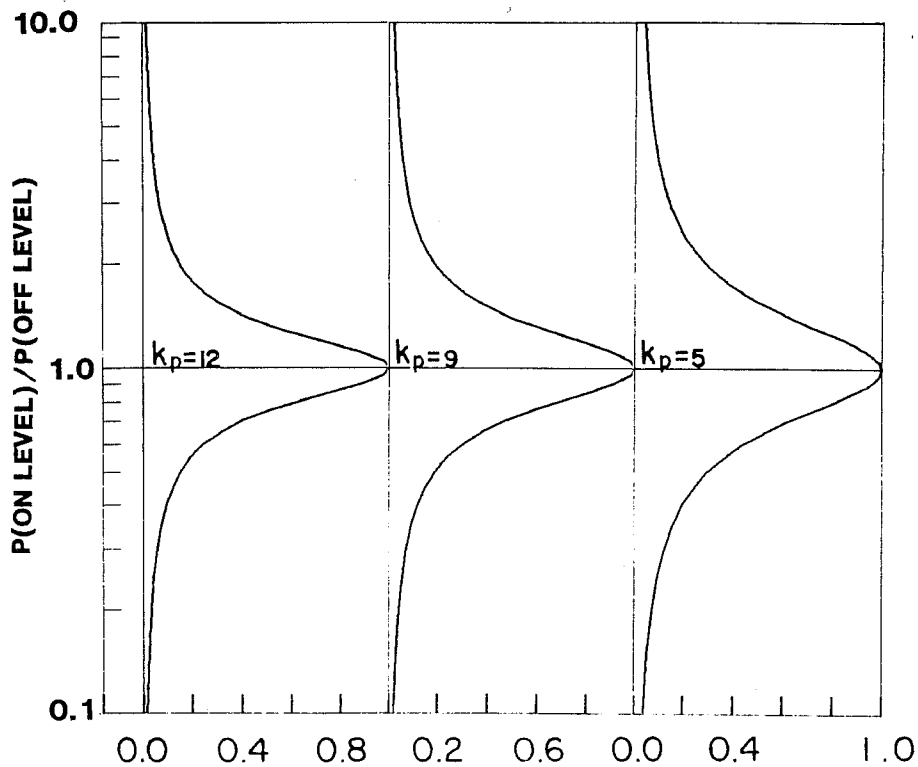


Figure 7. Vertical first guess error correlation for selected values of  $k_p$ .

of all single level data being selected. This improves the vertical consistency of the analysis because the same profile reports tend to be selected at each level. The restrictions on the number of values from individual profile reports insures that the analysis will not be monopolized by values from reports which are nearly coincident with the grid point. The selection for both profile and single-level reports is based on proximity with the grid point as determined by the three-dimensional first guess error autocorrelation for height. The values of  $k_h$  and  $k_p$  are fixed for this calculation and are the same as those given for the 1000 mb analysis.

The weights,  $w_i$ , for the observed corrections are calculated next by solving the matrix problem represented by Equation (2.2). Values pertinent to the calculation of the matrix elements discussed below are listed in Table 5. The variation of the horizontal and vertical correlation of hh is depicted in Figs. 6 and 7 for selected values of  $k_h$  and  $k_p$ . The GOI uses values of  $k_p = 5$  and  $k_h = 2. \times 10^{-6} \text{ km}^{-2}$ .

Table 5. Parameters used in the calculation of elements of Equation 2.2

Analysis Level	$k_h$ $\times 10^{-6} \text{ km}^{-2}$	$k_p$	N	DF	EF
1000 mb h	3.000	9	16	NA	NA
1	4.125	9 (12)	36	.50	.50
2	3.750	9	33	.65	.65
3	3.375	9	30	.80	.80
4	3.125	9	30	.95	.95
5-12	3.000	9	30	1.00	1.00
13	3.000	9	30	.95	1.00
14	3.000	9	30	.80	1.05
15	2.250	9	30	.65	1.25
16	1.500	9	30	.50	1.50
1-12 q	3.750	4-14	10	NA	NA

The horizontal correlations (see Figure 6) used by the ROI have a steeper slope than those used in the GOI. This reflects the finer resolution of the ROI analysis grid. The extra resolution translated into 'error' at wave numbers higher than the 30 waves of the spectral model used in the GDAS. If a complete power spectrum of forecast error were integrated to obtain an isotropic structure function for the error, a sharper curve would result than if the spectrum were truncated first to the resolution of the forecast. This has not actually been done, but the basic premise still remains. Clearly, the ROI can resolve finer scales in the correction field, but only if the implied scale of the correlation model is decreased. This argument is applicable to the vertical correlation function (see Figure 7), which is also sharper than the one used by the GOI.

The horizontal correlation varies with analysis level. This is also done in the GOI, but only at the top two levels, 70 mb and 50 mb, where the function becomes broader. We have extended this variation to the first four levels (through the first 150 mb). This reflects the presence of smaller scales in the corrections observed near the surface. The factor DF in Table 5, refers to a decoupling factor. This factor is used to multiply all cross-correlations involving geopotential and wind. It weakens, but does not eliminate, the geostrophic coupling of the mass and wind correction fields. This affects the off-diagonal terms on the left hand side of the matrix (2.2) as well as the right hand side. In the lowest levels, this is a reflection of the frictional and boundary-layer effects which act to produce ageostrophic flow. In the upper levels, it is a reflection of our distrust of the geopotential corrections, which contain detrimental effects due to first-guess biases and integrated observational errors. It was found, that a strict geostrophic application in the presence of very large geopotential corrections resulted in correspondingly and unmeteorolo-

logically large wind corrections. The partial decoupling resulted in more reasonable results.

The adjustments made in the lowest and highest levels affect the off-diagonal terms. An adjustment of the diagonal terms is also made. From 2.2, the diagonal terms on the left hand side involve the correlation of an observed correction with itself, which is unity, plus a term representing the ratio of the standard deviation of the observational error to that of the first-guess error. This error ratio for wind corrections only is divided by the factor EF listed in Table 5. Where the factor is less than unity, the error ratio is increased and the correction receives a reduced weight in the analysis (2.1) and vice versa. Based on the arguments made above, we choose to believe wind reports more than height reports at the highest levels and we choose to believe height reports more than wind reports at the lowest levels.

The observational error is generally considered to be made up to two contributions. The first is the measurement error inherent in the instrument. The second is an error of representativeness. The latter is a function of the resolution of the analysis. The finer the analysis the closer the specified observational error becomes to the actual instrument error. The base values of observational error standard deviation are the same as those given in Dey and Morone (1985) and used in the GOI. However, because the ROI is performed on a finer grid both vertically and horizontally compared to the GOI, these values are reduced in the ROI. The reduction factor which is applied to a particular observed correction depends on the quality code and on whether the correction was flagged as large in the GROSS check (see Table 4). The reduction factors used are listed in Table 6.



Table 6. ROI reduction factors applied to the GOI observational error standard deviations

Code	Unflagged	Flagged
0	.25	.20
1	.50	.45
2	.60	.55
3	.80	.75

Note that the amount of reduction is slightly greater for the flagged reports. This will reduce the error ratio and increase the weight given the report in the analysis. It is argued that since the report has survived the quality checks, it is reliable. The fact that its magnitude is large suggests that the first-guess is 'incorrect' in the vicinity of the report. Giving these reports increased weight allows the analysis to correct this region of the first guess more than would otherwise be the case.

At this point, the treatment of surface mass corrections of both geopotential and temperature will be addressed. At the first analysis level (the first sigma interface at the terrain level), the geopotential corrections from surface reports are used directly. These were constructed from the surface (station) pressure and the elevation of the station. In general, surface reports selected for the first level will also be selected for the analysis at the second and subsequent (up to five) levels. When this occurs, the height correction is adjusted using the surface temperature correction. The adjustment consists of converting the temperature correction into a thickness correction. The conversion assumes the temperature is valid over a shallow layer. The thickness correction is added to the surface height correction. This effectively raises the height correction to the top of the layer. The report pressure is similarly adjusted by adding the layer depth used in the conversion. At the second level a depth of 20 mb is used. At level three and above, a fixed depth of 40 mb is

used. This process amounts to generating a mini profile consisting of the surface value and two extrapolated values separated by 20 mb between each level. A sharper vertical correlation ( $k_p = 12$ ) is used when any form of surface data is used.

Once the  $h$ ,  $u$  and  $v$  corrections are calculated at all levels at a point, the moisture field is analyzed. First, the local profiles of the first guess mass and wind fields at the point are corrected. These are preliminary analysis fields of  $T_v$ ,  $u$  and  $v$  because they have not been adjusted for the new surface pressure which is done in the UPDATE step. The  $T_v$  corrections at sigma mid-points are obtained by differentiating the profile of  $h$  corrections. Wind corrections are simply averaged to the mid-points.

The preliminary analyses are used in a similar manner as described by Dey and Morone (1985) to prescribe the first guess error correlation model for specific humidity. The horizontal part of the correlation depends on the wind direction and speed. It is elliptical with the major axis rotated to be along the direction of the wind. If the wind speed is less than  $3.1 \text{ ms}^{-1}$ , the function is circular. For stronger wind speeds, the ellipse becomes more elongated. An example is provided in Figure 8. The GOI procedure simply reduces the effective distance in the direction of the minor axis. This shrinks the area covered by a given contour of correlation. In the ROI, the area will actually increase as the wind speed increases,  $k_h$  is allowed to decrease to a value of  $1.875 \times 10^{-6} \text{ km}^{-2}$ . The vertical correlation is a function of the lapse rate or stability. The GOI adjusts  $k_p$  upwards under stable conditions to become sharper which limits the vertical extent of a report's influence. The ROI allows adjustment of  $k_p$  both upwards to a value of 14 under stable conditions as well as downwards to a value of 4 in unstable conditions when vertical mixing is likely to occur.

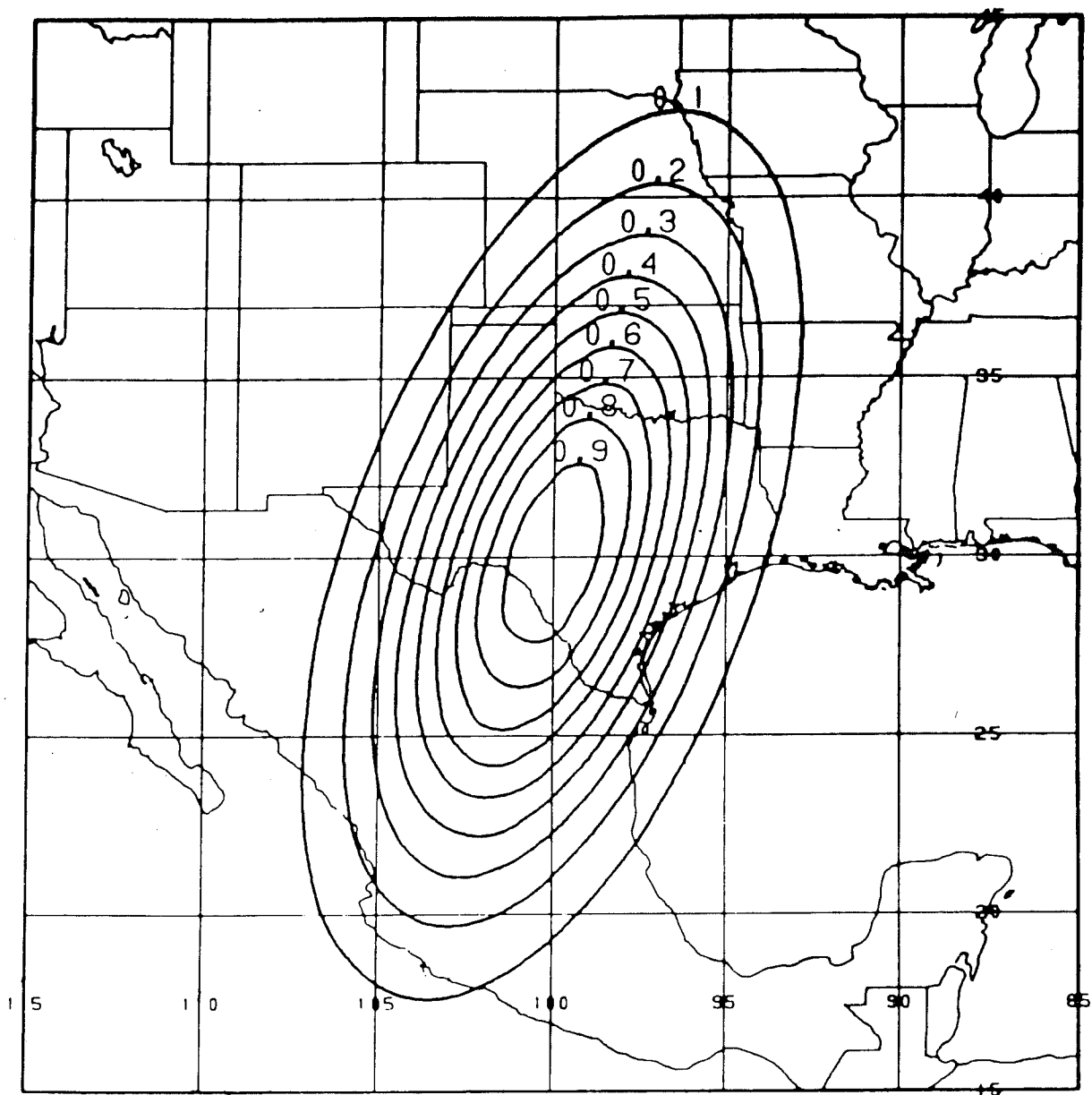


Figure 8. Example of horizontal forecast error correlation for specific humidity.

The analysis of moisture corrections proceeds as follows. The 10 'closest' reports are selected based on values of the adjusted correlation. Only the one closest report in the vertical is selected from any profile report. There is no partitioning of the 10 reports by category. The error ratio used in constructing the matrix (2.2) elements is calculated from the type and quality code of each report, i.e. the first guess error standard deviation and observational error standard deviation are not specified explicitly. This avoids the tricky problem of converting relative humidity errors and error growth rates into values for specific humidity.

Just prior to solving the matrix for the weights, a final adjustment of the error ratio term is made. All radiosonde reports with values of 0.85 forecast error correlation or greater are averaged together. This is a preliminary estimate of the correction based on the closest and most reliable sources of moisture information. All remaining corrections with correlation values less than 0.85 which deviate in sign or deviate significantly in magnitude from the core value, have their error ratios increased to a value of 2.5, which severely reduces their impact on the solution at this point. If there are no radiosonde reports within 0.85 correlation, then no final adjustment is made. This procedure can be thought of as a means of quality controlling the moisture data. Specific humidity corrections are not checked for horizontal consistency in the 'buddy' check and are checked against a fixed value which does not even vary with pressure in the 'gross' check.

When all h, u, v and q corrections are calculated on the thinned grid, they are interpolated back to the full 180 x 60 ROI grid and passed on to the UPDATE step (Figure 3). Prior to processing, the wind corrections are interpolated to the sigma mid-points assuming linear variation with respect

to  $p$ . A light, 25-point filter is then applied to the horizontal correction field for all variables. Next, a value of the new surface pressure,  $P^*$ , is computed. This involves a hydrostatic conversion of the first level height correction, which is valid at the first guess  $P^*$ , to a surface pressure correction. This 'analyzed' value of the surface pressure is obtained by correcting the first guess value.

Treatment of the mass field variables follows the same procedure discussed in Section 3.6. The first guess geopotential field at the original sigma interfaces is generated by integrating the first-guess mid-point temperatures. The corrections which were generated at the original sigma interfaces are then added to the first guess. Distribution of the heights to the new sigma structure based on the new surface pressure is achieved by interpolation using the AITKEN iterated technique. Mid-point and interface values are generated to allow the same adiabatic check to be performed. As before, the mid-point geopotentials are extracted and mid-point virtual temperatures are generated by differentiating the checked height profile.

The moisture and wind field corrections are applied directly to the first guess mid-point values. With surface pressure changes of only 2-6 mb, the extra effort to interpolate the corrections to the new mid-points did not seem necessary. The analysis fields of  $P^*$ ,  $T_v$ ,  $u$ ,  $v$  and  $q$  plus the terrain field are provided to the initialization code in the form of spherical harmonics (subject to an equatorial symmetry condition). The same fields plus the geopotentials are put out in the same strip form as the first guess. These fields are post-processed to pressure surfaces in the vertical and to the LFM grid in the horizontal for transmission back to the frontend computer for display, verification and archiving.

## 6. PERFORMANCE CHARACTERISTICS

Figure 9 summarizes the analysis verification statistics relative to radiosonde data over North America. Results are presented for the month of May 1985 for the LFM (early), the ROI (regional) and the GOI (aviation) analyses. All three use the same first guess fields from the GDAS. However, the LFM uses only the 1000 and 300 mb level heights directly, generating the other 'first guess' fields by computation from analyses at those levels. Verification plots for the initialized ROI analyses are not yet available.

In general, the ROI analysis falls between the LFM and the GOI in terms of goodness of fit against observations. This is the expected result. The LFM performs univariate analyses on mandatory surfaces and essentially will replace the first guess with a blend of the observations where data are plentiful. It is a 'credible' analysis in that it draws for the data. The ROI is multivariate and three-dimensional and allows implicitly for some weight to be given to the first guess. The latter is true even in the presence of high quality data. The GOI fit to the data is looser than the ROI primarily because the observational error standard deviations have been reduced in the ROI. This means that the GOI gives the data less weight relative to the first guess than the ROI, and vice versa.

The only significant feature of the mean statistics is the apparent tendency of the ROI to underestimate the wind speed at 250 mb. This, we feel, is due to the fairly sparse vertical resolution of the ROI sigma structure (see Figure 2) near this level. Both the LFM and GOI are performed and verified at 250 mb, whereas the ROI is performed at sigma points separated by 70 mb near this level. The mid-point analyses must also be interpolated in the vertical to the 250 mb verification level. Significantly, the

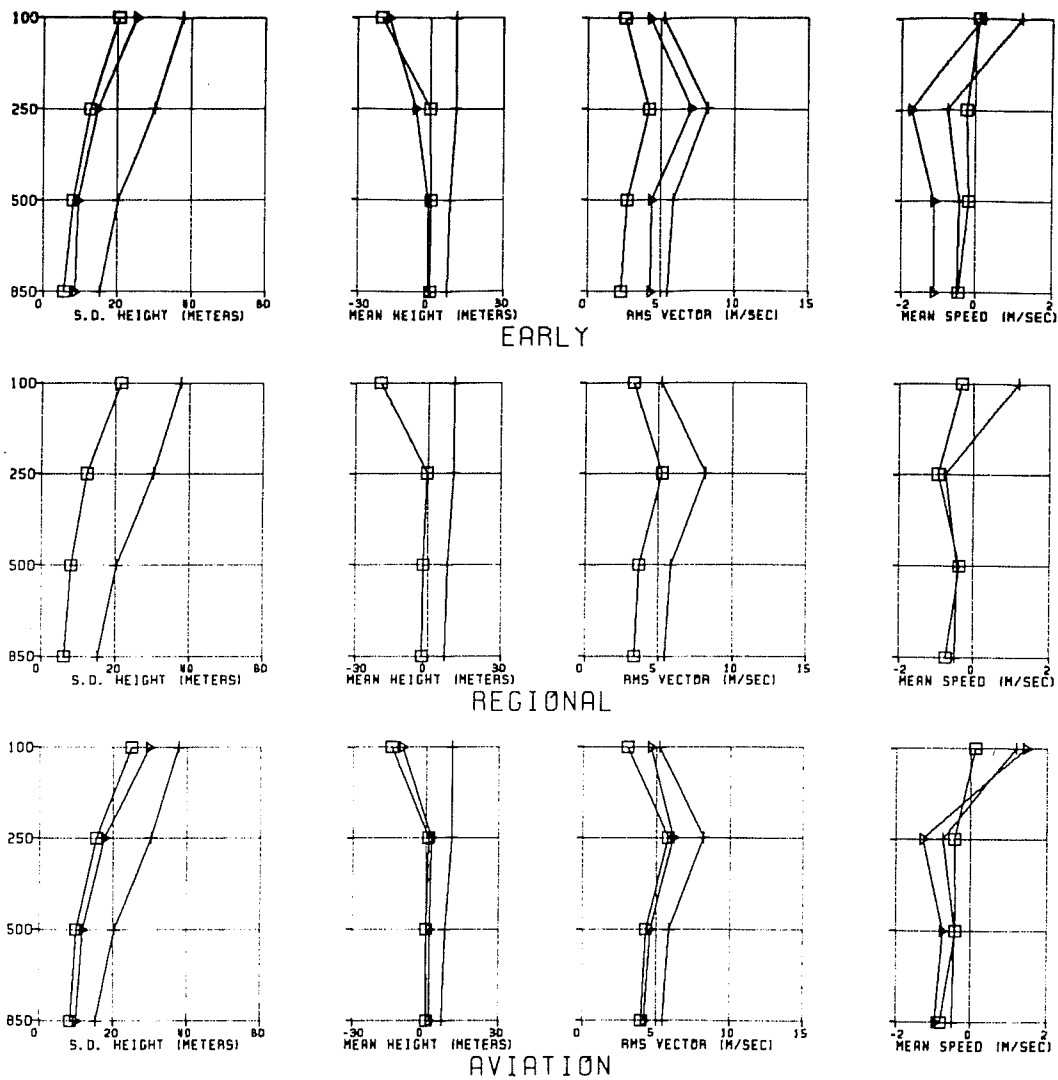


Figure 9. Mean and standard deviation (SD) of height and wind fit of first guess (+), analysis ( $\square$ ) and initialization ( $\triangleright$ ) to North American radiosonde data for early run (LFM, top), regional run (ROI, center) and aviation run (GOI, bottom) for May 1985.

initialized statistics for the LFM and GOI, a process which necessitates interpolation into the sigma coordinate and back to pressure, exhibit larger wind speed biases than the ROI analysis. Selected comparisons of difference fields between the initialized and analyzed ROI suggest that the differences are fairly small and not systematic.

Turning our attention next to the moisture field, Figure 10 presents a vertical cross-section of relative humidity for the ROI analysis, the LFM analysis and the first guess. The cross-section runs north to south along 98W through the central United States. The LFM analysis, which is of precipitable water in only the lowest three sigma layers, can capture only the grossest features. The first guess is only slightly more detailed. On the other hand, the ROI displays considerable detail in both the horizontal and vertical directions. By way of verification, the approximate location of Dallas-Fort Worth Texas is indicated by DFW. The analysis has represented a distinct double maxima in the profile above this point. The observed radiosonde profile at this station is presented in Figure 11, together with the interpolated profiles from the ROI, LFM and first guess fields. The LFM and first guess profiles are simply too smooth. The ROI, however, has quite faithfully reproduced the observed profile of dew-point and degree of saturation as well as the temperature.

The ultimate criterion for evaluating the performance of an analysis system designed to provide initial conditions for a forecast is the verification of those forecasts. Accordingly, Figure 12 shows the daily variation of the 500 mb height anomaly correlation for 48 hour forecasts from the RAFS and the LFM for the months of April and May 1985. Clearly, the majority of cases show the RAFS outperforming the LFM in April 1985. The situation in May 1985 is not nearly as clear. One impression stands out during both



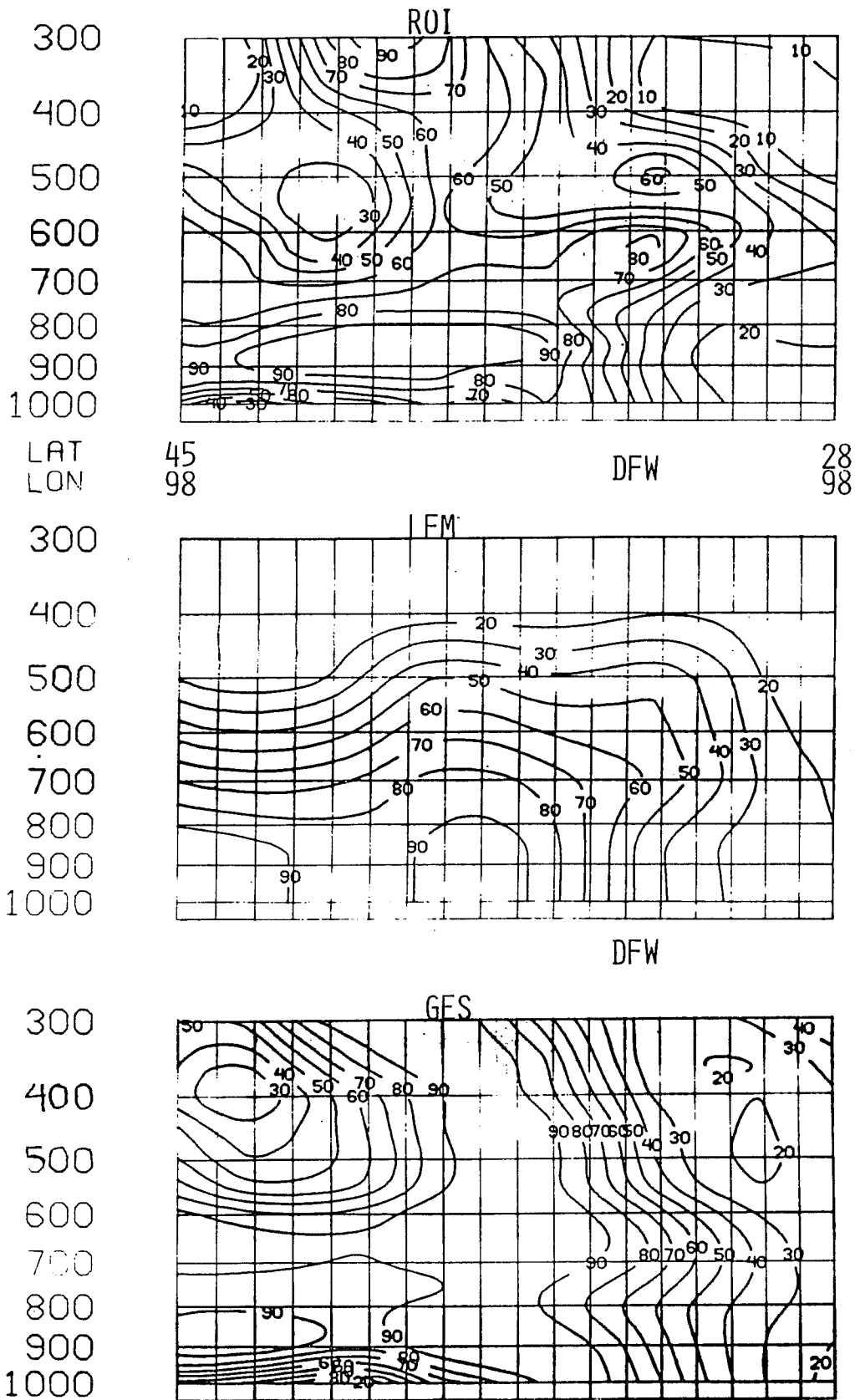


Figure 10. Vertical cross-section of relative humidity (%) for 0000 GMT 28 March 1984 for ROI analysis (top), LFM analysis (center) and first guess (bottom). DFW refers to location of Dallas-Fort Worth, Texas.

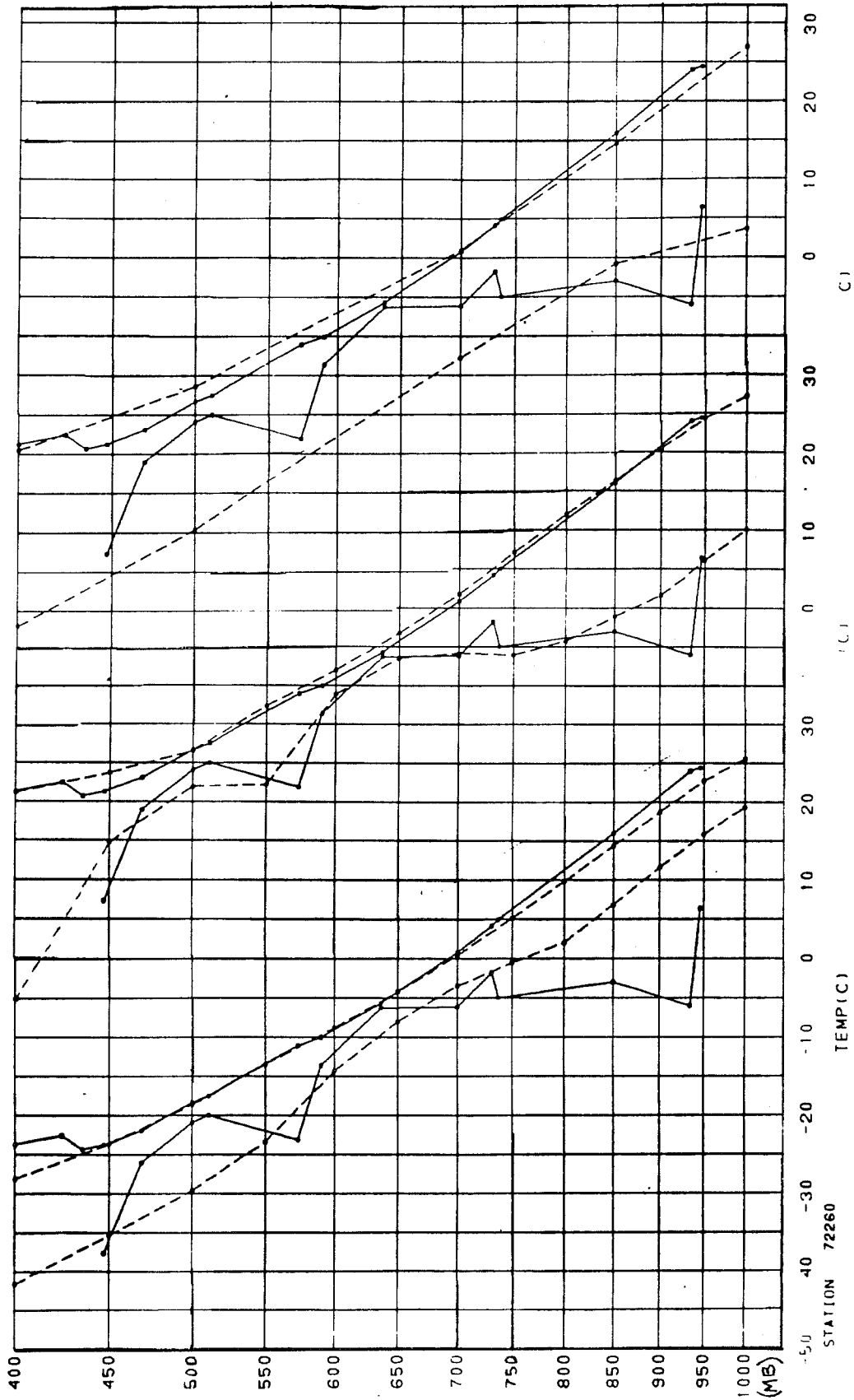


Figure 11. Plot of temperature and dew point profile from radiosonde ascent (solid) at Dallas-Fort Worth for 0000 GMT 28 March 1984. Profiles repeated three times, temperature scale overlaps. Dashed curves represent first guess (left), ROI analysis (center) and LFM analysis (right) interpolated to report location.

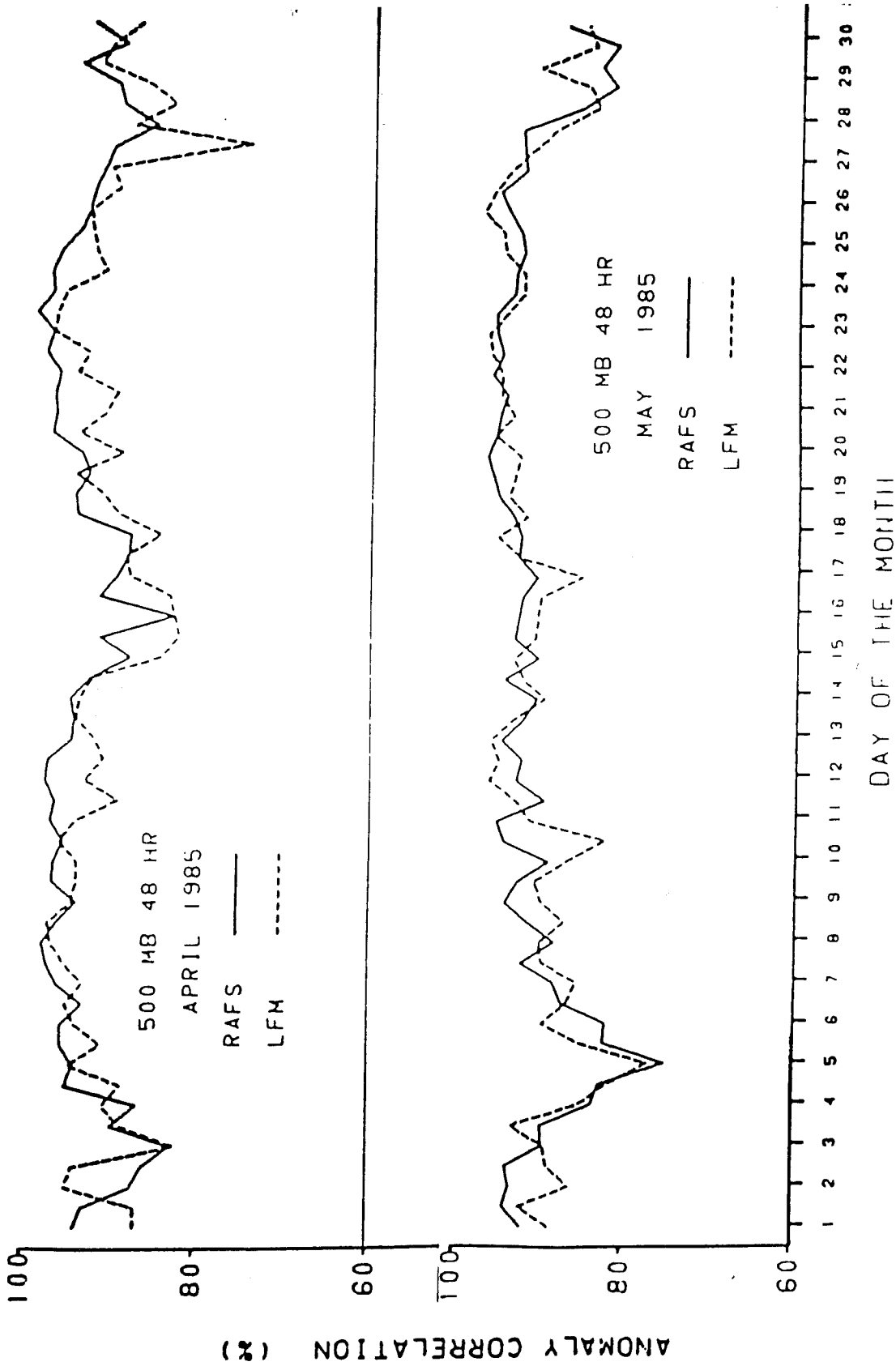


Figure 12. Daily variation of 48 hour 500 mb height anomaly correlation.

months. The RAFS performance appears more consistent and less variable than the LFM. Another indication of the quality of the new analysis system has come from several experimental forecasts with the operational LFM model run from initial conditions specified from the ROI analyses. Every experimental run has been either as good or better than the operational LFM forecast run from the LFM analyses.

## 7. SUMMARY

The new NMC regional analysis system has been described. Building upon the existing experience and methodology at NMC, it has met its pre-defined goals and has extended the application of optimum interpolation techniques to a finer scale. Among its unique aspects are:

- hemispheric domain
- regional scale resolution
- improved vertical resolution
- sigma vertical coordinate
- high-resolution terrain
- multivariate in h, u and v in sigma
- treatment of first guess in sigma
- treatment of significant level data
- treatment of surface data
- treatment of 'super' observations
- increased dependence on quality codes
- reduced observational error standard deviations
- sharper and more variable correlation functions
- increased detail in the analyses.

Many improvements await testing and implementation in both the analysis and the prediction model.

## REFERENCES

- Baer, F. and J. Tribbia, 1977: On complete filtering of gravity modes through non-linear initialization. *Mon. Wea. Rev.*, 105, 1536-1539.
- Beckman, F. S., 1960: The solution of linear equations by the conjugate gradient method. *Mathematical Methods for Digital Computers*, Vol. 1, A-Rolston and H. S. Wilf, Eds., Wiley, 62-72.
- Bergman, K., 1979: Multivariate analysis of temperature and winds using optimum interpolation. *Mon. Wea. Rev.*, 107, 1423-1444.
- Conte, S. D., 1965: *Elementary numerical analysis*. McGraw Hill, 278 pp.
- Cressman, G., 1959: An operational objective analysis system. *Mon. Wea. Rev.*, 87, 367-374.
- Dey, C. H. and L. L. Morone, 1985: Evaluation of the National Meteorological Center global data assimilation system: January 1982-December 1983. *Mon. Wea. Rev.*, 113, 304-318.
- DiMego, G., P. Phoebus and J. McDonell, 1985: Data preprocessing and quality control for optimum interpolation analysis at the National Meteorological Center. NMC Office Note 306. [Available from NMC, 5200 Auth Road, Washington, DC 20233.]
- Gerrity, J., 1977: The LFM model--1976: A documentation. NOAA Tech. Memo. NWS NMC 60, 68 pp.
- Lorenc, A. C. 1981: A global three-dimensional multivariate statistical interpolation scheme. *Mon. Wea. Rev.*, 109, 701-721.
- Hoke, J., 1984: Forecast results for NMC's new regional analysis and forecast system. Preprints, Tenth Conference on Weather Forecasting and Analysis, Clearwater Beach, Florida, June 25-29, 1984, 418-423.
- McInturff, R. M., F. G. Finger, K. M. Johnson and J. D. Laver, 1979: Day-night differences in radiosonde observations of the stratosphere and troposphere. NOAA Tech. Memo. NWS NMC 63, 47 pp.

Phillips, N., 1979: The nested grid model. NOAA Tech. Report, NWS 22,  
80 pp.

Sela, J. G., 1980: Spectral modeling at the National Meteorological  
Center. Mon. Wea. Rev., 103, 246-257.